To: Computers and Structures

Substructure Based Approach to Finite Element Model Updating

Shun Weng
Ph. D student,
Department of Civil and Structural Engineering,
The Hong Kong Polytechnic University,
Hung Hom, Kowloon, Hong Kong
Tel: (852) 2766 4485; Fax: (852) 2334 6389
06901937r@polyu.edu.hk

School of Civil Engineering and Mechanics,
Huazhong University of Science and Technology,
Wuhan, Hubei, P. R. China

Yong Xia*
Assistant Professor,
Department of Civil and Structural Engineering,
The Hong Kong Polytechnic University,
Hung Hom, Kowloon, Hong Kong
Tel: (852) 2766 6066; Fax: (852) 2334 6389
ceyxia@polyu.edu.hk

You-Lin Xu
Chair Professor,
Department of Civil and Structural Engineering,
The Hong Kong Polytechnic University,
Hung Hom, Kowloon, Hong Kong
Tel: (852) 2766 6050; Fax: (852) 2334 6389
ceylxu@polyu.edu.hk

Hong-Ping Zhu
Professor,
School of Civil Engineering and Mechanics,
Huazhong University of Science and Technology,
Wuhan, Hubei, P. R. China
Tel: (86) 27 87542631
hpzhu@mail.hust.edu.cn

(* Corresponding author)

Substructure Based Approach to Finite Element Model Updating

ABSTRACT

A substructure-based finite element model updating technique is proposed in this paper. A few eigenmodes of the independent substructures and their associated derivative matrices are assembled into a reduced eigenequation to recover the eigensolutions and eigensensitivities of the global structure. Consequently, only the concerned substructures and the reduced eigenequation are re-analyzed in the optimization process, thus reducing the computational load of the traditional model updating methods which perform on the global structure. Applications of the proposed substructure-based model updating to a frame structure and a practical bridge demonstrate that the present method is computationally effective and efficient.

Keywords: Model updating; Substructuring; Eigensolution; Eigensensitivity

Nomenclature

K, M	Stiffness matrix, mass matrix
λ_i, $\mathbf{\Lambda}$	The i^{th} eigenvalue, matrix of eigenvalues
ϕ_i, $\mathbf{\Phi}$	The i^{th} eigenvector (mode shape), matrix of eigenvectors
$\bar{\mathbf{\Phi}}$	Matrix of expanded mode shapes
J	Objective function
S	Sensitivity matrix
r	Elemental physical parameter
τ	Interface force along the boundaries of the substructures
$\mathbf{C}$	Connection matrix
N	Degrees of freedom of the global structure
N_S	Number of the independent substructures
NP	Size of the primitive matrix, or the degrees of freedom of all substructures
$n^{(j)}$	Degrees of freedom of the jth substructure
$\mathbf{z}$	Participation factor of the substructural eigenmodes

Superscripts

(j)	The jth substructure
p	Primitive matrix or vector
T	Transpose of matrix or vector

Subscripts

m	Master modes
s	Slave modes
i	The ith modes

1. Introduction

Accurate finite element (FE) models are frequently required in a large number of applications, such as optimization design, damage identification, structural control and structural health monitoring [1]. Due to uncertainties in the geometry, material properties and boundary conditions, the dynamic responses of a structure predicted by a highly idealized numerical model usually differ from the measured responses. For example, Brownjohn et al. [2] reported that the differences between the experimental and numerical modal frequencies of a curved cable-stayed bridge exceeded 10% for most modes and even reached 40% in some cases. In another study [3], 18% difference was found between the analytical and measured frequencies. Jaishi and Ren [4] observed differences of up to 20% in the natural frequencies predicted by an FE model and those measured in a steel arch bridge, and reported that the Modal Assurance Criteria (MAC) values could be as low as 62%. Similarly, Zivanovic et al. [5] found that the natural frequencies of a footbridge predicted by an FE model in the design before updating differed from their experimental counterparts by 29.8%. Therefore, an effective model updating method is necessary to obtain a more accurate FE model that can be used for other purposes such as prediction of response and damage identification.

Model updating methods are usually classified into two categories: one-step methods and iterative methods [6]. The former directly reconstruct the stiffness and mass matrices of the analytical model, while the latter modify the physical parameters of the FE model repeatedly to minimize the

discrepancy between the analytical modal properties (frequencies and mode shapes) and the measurement counterparts. The iterative methods are becoming more popular, since they allow for the physical meaning of the predicted parameters to be reflected, and the symmetry, positive-definiteness and sparseness in the updated matrices to be preserved.

Most iterative model updating methods employ optimization techniques, which require the eigensolutions and associated sensitivity matrices of the analytical model to be calculated in each iteration [7]. As the analytical model of a practical structure in civil engineering usually comprises a large number of degrees of freedom (DOFs) and contains many uncertain parameters that need to be updated, extracting the eigensolutions and associated eigensensitivities from the large-size system matrices is very time-consuming.

The substructuring method is preferable to cope with large scale structures. In general, the individual substructures are analyzed independently to obtain designated solutions, which are subsequently assembled to recover the properties of the global structure by constraining the interfaces of the adjacent substructures [8]. The substructuring method is advantageous mainly in three aspects. First, as the global structure is replaced by smaller and more manageable substructures, it is much easier and quicker to analyze the small system matrices. Second, the separated substructures are analyzed independently. When one or more substructures are modified, only the modified substructures need

to be reanalyzed while the others remain unchanged [9]. This property can be promising when applied to model updating or damage identification field. When the uncertain parameters or the damage areas are localized within parts of a structure, only one or more substructures containing those parts are re-analyzed during model updating or damage identification, and the other substructures are untouched [10, 11]. The substructuring method will be more efficient when some identical substructures exist or when the substructuring method is incorporated with parallel computation. Finally, the substructuring method is helpful to be combined with the model reduction technique in calculating the eigensolutions and eigensensitivities [12, 13].

Kron [14] first proposed a substructuring method to study the eigensolutions of large scale systems in a piecewise manner, and it has been developed by the authors in terms of efficiency [15, 16]. This paper attempts to extend the substructuring method to calculate the eigensolutions and eigensensitivities for the sensitivity-based model updating process. The eigensolutions and eigensensitivities of the global structure are recovered from a few eigenmodes and their associated derivatives of the independent substructures. In particular, eigensensitivity with respect to an elemental parameter of the global structure is calculated from the derivative matrices of one substructure that contains the element. The derivatives of other substructures to the elemental parameter are zero. This can save a large amount of computational effort in calculation of the eigensolutions and eigensensitivities which dominate the model updating process. The effectiveness

and efficiency of the proposed method are illustrated through a numerical frame structure and a practical bridge.

2. Sensitivity-based model updating method

In sensitivity-based model updating procedure, the general objective function combining the modal properties of the frequencies and mode shapes is usually denoted as [6]

$$J(r)=\sum_i W_{\lambda i}^2\left[\lambda_i\left(\{r\}\right)^A-\lambda_i{}^E\right]^2+\sum_i W_{\phi i}^2\sum_j\left[\phi_{ji}\left(\{r\}\right)^A-\phi_{ji}{}^E\right]^2 \tag{1}$$

where $\lambda_i{}^E$ represents the eigenvalue which is the square of the *i*th experimental frequency, $\phi_{ji}{}^E$ is the *i*th experimental mode shape at the *j*th point. $\lambda_i{}^A$ and $\phi_{ji}{}^A$ denote the corresponding eigenvalue and mode shape from the analytical FE model, which are expressed as the function of the uncertain physical parameters $\{r\}$. $W_{\lambda i}$ and $W_{\phi i}$ are the weight coefficients due to the different measurement accuracy of the frequencies and mode shapes. The objective function is minimized by continuously adjusting the parameters $\{r\}$ of the initial FE model through optimization searching techniques.

The optimization algorithm, which is a sensitivity-based iterative procedure, minimizes the objective function in a trust region. The quadratic model $Z(r)$ is defined by a truncated Taylor series of $J(r)$ as [7, 17]

$$Z(r) = J(r) + \left[\nabla J(r)\right]^{\mathrm{T}} \{\Delta r\} + \frac{1}{2}\{\Delta r\}^{\mathrm{T}} \left[\nabla^2 J(r)\right]\{\Delta r\} \tag{2}$$

where $\{\Delta r\}$ denotes a step vector from the current $\{r\}$. $\nabla J(r)$ and $\nabla^2 J(r)$ are the gradient and the Hessian of $J(r)$, respectively. After an iterative process, the optimized $\{r^*\}$ is reached with $\nabla J(r) \approx 0$. The gradient and Hessian of $J(r)$ can be expressed by the sensitivity matrix as

$$\nabla J(r) = \left[S(r)\right]^{\mathrm{T}} \{2 f(r)\}, \ \nabla^2 J(r) \approx S(r)^{\mathrm{T}} S(r) \tag{3}$$

where $\{f(r)\}$ encloses the weighted residuals $W_\lambda\left(\lambda\left(\{r\}\right)^A - \lambda^E\right)$ and $W_\phi\left(\phi\left(\{r\}\right)^A - \phi^E\right)$. In each iteration, the optimization algorithm constructs a model function $Z(r)$ near the current point $\{r\}$ according to the sensitivity matrix, and determines a trust region surrounding the current $\{r\}$. The optimized value of $\{r^*\}$ in this iteration is then computed by minimizing the model function $Z(r)$ inside the trust region.

To find the optimal searching direction, sensitivity analysis is usually conducted to compute the rate of the change of a particular response quantity with respect to the change in a physical parameter [7]. For example, the sensitivity matrices of the eigenvalues and mode shapes with respect to a parameter *r* can be expressed as

$$\left[S_\lambda(r)\right] = \frac{\partial \lambda(r)}{\partial r}, \ \left[S_\phi(r)\right] = \frac{\partial \phi(r)}{\partial r} \tag{4}$$

[*S*(*r*)] can be computed for all elemental parameters using the finite difference method, modal method or Nelson's method. The finite difference method calculates the eigensolutions at perturbed points and compares the differences at these points as the derivative [17]. This method is sensitive to the round off and truncation errors associated with the step size used and is computationally

inefficient, so it is usually not employed for model updating. Fox and Kappor [19] proposed the modal method, which approximated the eigenvector derivatives as a linear combination of the eigenvectors. As all modes of the system are required to calculate the eigenvalue and eigenvector derivatives, this method was computationally expensive for a large-scale structure. Nelson's method [19] calculates the eigenvector derivative using the modal data of that mode solely. It is exact and computationally efficient. Sutter et al. [20] compared the difference method, modal method and Nelson's method in terms of computational accuracy and efficiency, and concluded that the Nelson's method is the most powerful one among the three methods. Hence, Nelson's method will be considered in this research to be integrated with the substructuring method for eigensensitivities.

In traditional model updating methods, the eigensolutions and eigensensitivity matrices are calculated from the system matrices of the global structure, based on the classical eigenequation

$$\mathbf{K}\{\phi_i\} = \lambda_i \mathbf{M}\{\phi_i\} \tag{5}$$

where **K** and **M** are the stiffness and mass matrices, and λ_i and $\{\phi_i\}$ are the *i*th eigenvalue and eigenvector, respectively. Based on Eq. (5), the Lanczos method or Subspace Iteration method are widely employed to calculate the eigensolutions for a large-scale structure, while the Nelson's method is used for the eigensensitivity [21]. These traditional methods calculate the eigensolutions and eigensensitivity by treating the entire structure as a whole. Updating the FE model of a large-scale structure usually involves a heavy workload, as calculating the eigensolutions and

eigensensitivities based on the large-size system matrices is expensive and many runs are usually required to achieve the convergence of the optimization. To reduce this computational burden, in the present paper, a structure is divided into a few independent substructures whose eigensolutions and eigensensitivity are analyzed independently. The substructural solutions are then assembled to obtain the eigensolutions and eigensensitivity of the global structure by imposing constraints on them. The substructuring method is proposed in the following sections to estimate the eigensolutions and eigensensitivities for model updating purpose.

3. Eigensolutions with substructuring method

The global structure with N DOFs is divided into N_S substructures. Treating the jth substructure of $n^{(j)}$ DOFs (j=1, 2, …, N_S) as an independent structure, it has the stiffness matrix $\mathbf{K}^{(j)}$ and mass matrix $\mathbf{M}^{(j)}$, and $n^{(j)}$ pairs of eigenvalues and eigenvectors as [22]:

$$\mathbf{\Lambda}^{(j)} = \mathrm{Diag}\left[\lambda_1^{(j)}, \lambda_2^{(j)}, ..., \lambda_{n^{(j)}}^{(j)}\right], \quad \mathbf{\Phi}^{(j)} = \left[\phi_1^{(j)}, \phi_2^{(j)}, ..., \phi_{n^{(j)}}^{(j)}\right]$$

$$\left[\mathbf{\Phi}^{(j)}\right]^{\mathrm{T}} \mathbf{K}^{(j)} \mathbf{\Phi}^{(j)} = \mathbf{\Lambda}^{(j)}, \quad \left[\mathbf{\Phi}^{(j)}\right]^{\mathrm{T}} \mathbf{M}^{(j)} \mathbf{\Phi}^{(j)} = \mathbf{I}^{(j)}, \ (j=1, 2, \ldots, N_S) \tag{6}$$

Based on the principle of virtual work and geometric compatibility, Kron's substructuring method [14, 22] reconstructs the eigensolutions of the global structure by imposing the constraints at the interfaces as

$$\begin{bmatrix} \mathbf{\Lambda}^{\mathrm{p}} - \bar{\lambda}\mathbf{I} & -\mathbf{\Gamma} \\ -\mathbf{\Gamma}^{\mathrm{T}} & \mathbf{0} \end{bmatrix} \begin{Bmatrix} \mathbf{z} \\ \tau \end{Bmatrix} = \begin{Bmatrix} \mathbf{0} \\ \mathbf{0} \end{Bmatrix} \tag{7}$$

In this equation,

$$\boldsymbol{\Gamma} = \left[\mathbf{C}\boldsymbol{\Phi}^{\mathrm{p}} \right]^{\mathrm{T}},$$

$$\boldsymbol{\Lambda}^{\mathrm{p}} = \mathrm{Diag}\left[\boldsymbol{\Lambda}^{(1)}, \boldsymbol{\Lambda}^{(2)}, ..., \boldsymbol{\Lambda}^{(N_S)} \right], \quad \boldsymbol{\Phi}^{\mathrm{p}} = \mathrm{Diag}\left[\boldsymbol{\Phi}^{(1)}, \boldsymbol{\Phi}^{(2)}, ..., \boldsymbol{\Phi}^{(N_S)} \right], \tag{8}$$

where **C** is a rectangular connection matrix constraining the interface DOFs of the adjacent substructures to move jointly [23]. In matrix **C**, each row only contains two non-zero elements, which are 1 and -1 for rigid connection. τ is the internal connection forces of the adjacent substructures. $\bar{\lambda}$ is the eigenvalue of the global structure. **z** acts as the participation factor of the substructural eigenmodes, and the expanded eigenvectors of the global structure can be recovered by $\bar{\boldsymbol{\Phi}} = \boldsymbol{\Phi}^{\mathrm{p}} \{\mathbf{z}\}$. The eigenvector $\boldsymbol{\Phi}$ of the global structure is obtained by discarding the identical values in $\bar{\boldsymbol{\Phi}}$ at the interface points. Superscript 'p' denotes the diagonal assembly of the substructural matrices, representing the primitive matrices before constraining the independent substructures.

From the viewpoint of energy conservation, all modes of the substructures contribute to the eigenmodes of the global structure, i.e., the complete eigensolutions of all substructures are required to assemble the primitive form of $\boldsymbol{\Lambda}^{\mathrm{p}}$ and $\boldsymbol{\Phi}^{\mathrm{p}}$. It is inefficient and not worthwhile to calculate all modes of the substructures, as only a few eigenmodes are generally of interest for a large-scale structure. To overcome this difficulty, the proposed method will improve the efficiency of Kron's substructuring method by introducing a modal truncation technique. In each substructure, the first few eigensolutions, corresponding to the lower vibration modes, are selected as the 'master'

variables. The residual higher modes are treated as the 'slave' variables. Only the master modes are calculated to assemble the eigenequation of the global structure, while the slave modes are discarded in the later calculations. From here on, subscripts 'm' and 's' will denote the 'master' and 'slave' modes, respectively.

Assuming that the first $n_{\mathrm{m}}^{(j)}$ (j = 1, 2, …, N_S) modes in the jth substructure are chosen as the 'master' modes while the residual $n_{\mathrm{s}}^{(j)}$ higher modes are the 'slave' modes, the jth substructure has the 'master' eigenpairs and 'slave' eigenpairs as

$$\begin{aligned}
&\boldsymbol{\Lambda}_{\mathrm{m}}^{(j)} = \mathrm{Diag}\left[\lambda_1^{(j)}, \lambda_2^{(j)}, ..., \lambda_{n_{\mathrm{m}}^{(j)}}^{(j)}\right], \quad \boldsymbol{\Phi}_{\mathrm{m}}^{(j)} = \left[\boldsymbol{\phi}_1^{(j)}, \boldsymbol{\phi}_2^{(j)}, ..., \boldsymbol{\phi}_{n_{\mathrm{m}}^{(j)}}^{(j)}\right], \\
&\boldsymbol{\Lambda}_{\mathrm{s}}^{(j)} = \mathrm{Diag}\left[\lambda_{n_{\mathrm{m}}^{(j)}+1}^{(j)}, \lambda_{n_{\mathrm{m}}^{(j)}+2}^{(j)}, ..., \lambda_{n_{\mathrm{m}}^{(j)}+n_{\mathrm{s}}^{(j)}}^{(j)}\right], \quad \boldsymbol{\Phi}_{\mathrm{s}}^{(j)} = \left[\boldsymbol{\phi}_{n_{\mathrm{m}}^{(j)}+1}^{(j)}, \boldsymbol{\phi}_{n_{\mathrm{m}}^{(j)}+2}^{(j)}, ..., \boldsymbol{\phi}_{n_{\mathrm{m}}^{(j)}+n_{\mathrm{s}}^{(j)}}^{(j)}\right], \\
&n_{\mathrm{m}}^{(j)} + n_{\mathrm{s}}^{(j)} = n^{(j)}, \quad \left(j = 1, 2, ..., N_S\right)
\end{aligned} \tag{9}$$

Assembling the 'master' eigenpairs and 'slave' eigenpairs for all substructures, respectively, one has

$$\begin{aligned}
&\boldsymbol{\Lambda}_{\mathrm{m}}^{\mathrm{p}} = \mathrm{Diag}\left[\boldsymbol{\Lambda}_{\mathrm{m}}^{(1)}, \boldsymbol{\Lambda}_{\mathrm{m}}^{(2)}, ..., \boldsymbol{\Lambda}_{\mathrm{m}}^{(j)}, ..., \boldsymbol{\Lambda}_{\mathrm{m}}^{(N_S)}\right], \quad \boldsymbol{\Phi}_{\mathrm{m}}^{\mathrm{p}} = \mathrm{Diag}\left[\boldsymbol{\Phi}_{\mathrm{m}}^{(1)}, \boldsymbol{\Phi}_{\mathrm{m}}^{(2)}, ..., \boldsymbol{\Phi}_{\mathrm{m}}^{(j)}, ..., \boldsymbol{\Phi}_{\mathrm{m}}^{(N_S)}\right], \\
&\boldsymbol{\Lambda}_{\mathrm{s}}^{\mathrm{p}} = \mathrm{Diag}\left[\boldsymbol{\Lambda}_{\mathrm{s}}^{(1)}, \boldsymbol{\Lambda}_{\mathrm{s}}^{(2)}, ..., \boldsymbol{\Lambda}_{\mathrm{s}}^{(j)}, ..., \boldsymbol{\Lambda}_{\mathrm{s}}^{(N_S)}\right], \quad \boldsymbol{\Phi}_{\mathrm{s}}^{\mathrm{p}} = \mathrm{Diag}\left[\boldsymbol{\Phi}_{\mathrm{s}}^{(1)}, \boldsymbol{\Phi}_{\mathrm{s}}^{(2)}, ..., \boldsymbol{\Phi}_{\mathrm{s}}^{(j)}, ..., \boldsymbol{\Phi}_{\mathrm{s}}^{(N_S)}\right] \\
&NP_{\mathrm{m}} = \sum_{j=1}^{N_S} n_{\mathrm{m}}^{(j)}, \quad NP_{\mathrm{s}} = \sum_{j=1}^{N_S} n_{\mathrm{s}}^{(j)}, \quad NP = \sum_{j=1}^{N_S} n^{(j)}, \quad \left(j = 1, 2, ..., N_S\right)
\end{aligned} \tag{10}$$

Denoting $\boldsymbol{\Gamma}_{\mathrm{m}} = \left[\mathbf{C}\boldsymbol{\Phi}_{\mathrm{m}}^{\mathrm{p}}\right]^{\mathrm{T}}$, $\boldsymbol{\Gamma}_{\mathrm{s}} = \left[\mathbf{C}\boldsymbol{\Phi}_{\mathrm{s}}^{\mathrm{p}}\right]^{\mathrm{T}}$, the eigenequation (Eq. (7)) is re-written according to the master modes and slave modes as

$$\begin{bmatrix} \boldsymbol{\Lambda}_{\mathrm{m}}^{\mathrm{p}} - \bar{\lambda}\mathbf{I} & \mathbf{0} & -\boldsymbol{\Gamma}_{\mathrm{m}} \\ \mathbf{0} & \boldsymbol{\Lambda}_{\mathrm{s}}^{\mathrm{p}} - \bar{\lambda}\mathbf{I} & -\boldsymbol{\Gamma}_{\mathrm{s}} \\ -\boldsymbol{\Gamma}_{\mathrm{m}}^{\mathrm{T}} & -\boldsymbol{\Gamma}_{\mathrm{s}}^{\mathrm{T}} & \mathbf{0} \end{bmatrix} \begin{Bmatrix} \mathbf{z}_{\mathrm{m}} \\ \mathbf{z}_{\mathrm{s}} \\ \tau \end{Bmatrix} = \begin{Bmatrix} \mathbf{0} \\ \mathbf{0} \\ \mathbf{0} \end{Bmatrix} \tag{11}$$

With the second line of Eq. (11), the slave part of the mode participation factor can be expressed as

$$\mathbf{z}_{\mathrm{s}}=\left(\boldsymbol{\Lambda}_{\mathrm{s}}^{\mathrm{p}}-\bar{\lambda}\mathbf{I}\right)^{-1}\boldsymbol{\Gamma}_{\mathrm{s}}\tau \tag{12}$$

Substituting Eq. (12) into Eq. (11) gives

$$\begin{bmatrix}\boldsymbol{\Lambda}_{\mathrm{m}}^{\mathrm{p}}-\bar{\lambda}\mathbf{I} & -\boldsymbol{\Gamma}_{\mathrm{m}}\\ -\boldsymbol{\Gamma}_{\mathrm{m}}^{\mathrm{T}} & -\boldsymbol{\Gamma}_{\mathrm{s}}^{\mathrm{T}}\left(\boldsymbol{\Lambda}_{\mathrm{s}}^{\mathrm{p}}-\bar{\lambda}\mathbf{I}\right)^{-1}\boldsymbol{\Gamma}_{\mathrm{s}}\end{bmatrix}\begin{Bmatrix}\mathbf{z}_{\mathrm{m}}\\ \tau\end{Bmatrix}=\begin{Bmatrix}\mathbf{0}\\ \mathbf{0}\end{Bmatrix} \tag{13}$$

In Eq. (13), Taylor expansion of the nonlinear item $\left(\boldsymbol{\Lambda}_{\mathrm{s}}^{\mathrm{p}}-\bar{\lambda}\mathbf{I}\right)^{-1}$ gives

$$\left(\boldsymbol{\Lambda}_{\mathrm{s}}^{\mathrm{p}}-\bar{\lambda}\mathbf{I}\right)^{-1}=\left(\boldsymbol{\Lambda}_{\mathrm{s}}^{\mathrm{p}}\right)^{-1}+\bar{\lambda}\left(\boldsymbol{\Lambda}_{\mathrm{s}}^{\mathrm{p}}\right)^{-2}+\bar{\lambda}^{2}\left(\boldsymbol{\Lambda}_{\mathrm{s}}^{\mathrm{p}}\right)^{-3}+\cdots \tag{14}$$

In general, the required eigenvalues $\bar{\lambda}$ correspond to the lowest modes of the global structure, and are far less than the values in $\boldsymbol{\Lambda}_{\mathrm{s}}^{\mathrm{p}}$ when the master modes are appropriately chosen. In that case, retaining only the first item of the Taylor expansion gives $\boldsymbol{\Gamma}_{\mathrm{s}}^{\mathrm{T}}\left(\boldsymbol{\Lambda}_{\mathrm{s}}^{\mathrm{p}}-\bar{\lambda}\mathbf{I}\right)^{-1}\boldsymbol{\Gamma}_{\mathrm{s}}\approx\boldsymbol{\Gamma}_{\mathrm{s}}^{\mathrm{T}}\left(\boldsymbol{\Lambda}_{\mathrm{s}}^{\mathrm{p}}\right)^{-1}\boldsymbol{\Gamma}_{\mathrm{s}}$, and therefore Eq. (13) is simplified into

$$\begin{bmatrix}\boldsymbol{\Lambda}_{\mathrm{m}}^{\mathrm{p}}-\bar{\lambda}\mathbf{I} & -\boldsymbol{\Gamma}_{\mathrm{m}}\\ -\boldsymbol{\Gamma}_{\mathrm{m}}^{\mathrm{T}} & -\boldsymbol{\Gamma}_{\mathrm{s}}^{\mathrm{T}}\left(\boldsymbol{\Lambda}_{\mathrm{s}}^{\mathrm{p}}\right)^{-1}\boldsymbol{\Gamma}_{\mathrm{s}}\end{bmatrix}\begin{Bmatrix}\mathbf{z}_{\mathrm{m}}\\ \tau\end{Bmatrix}=\begin{Bmatrix}\mathbf{0}\\ \mathbf{0}\end{Bmatrix} \tag{15}$$

Representing τ with $\mathbf{z}_{\mathrm{m}}$ from the second line of Eq. (15) and substituting it into the first line, Eq. (15) is reduced into

$$\left[\left(\boldsymbol{\Lambda}_{\mathrm{m}}^{\mathrm{p}}-\bar{\lambda}\mathbf{I}_{\mathrm{m}}\right)+\boldsymbol{\Gamma}_{\mathrm{m}}\varsigma^{-1}\boldsymbol{\Gamma}_{\mathrm{m}}^{\mathrm{T}}\right]\mathbf{z}_{\mathrm{m}}=\mathbf{0}$$

$$\varsigma=\boldsymbol{\Gamma}_{\mathrm{s}}^{\mathrm{T}}\left(\boldsymbol{\Lambda}_{\mathrm{s}}^{\mathrm{p}}\right)^{-1}\boldsymbol{\Gamma}_{\mathrm{s}} \tag{16}$$

The size of the reduced eigenequation (Eq. (16)) is equal to the number of the retained master modes $NP_{\mathrm{m}}\times NP_{\mathrm{m}}$, which is much smaller than the original one of $NP\times NP$ in Eq. (7). $\bar{\lambda}$ and $\mathbf{z}_{\mathrm{m}}$ can be solved from this reduced eigenequation using common eigensolvers, such as Subspace Iteration or Lanczos method [21]. As before, the eigenvalues of the global structure are $\bar{\lambda}$, and the eigenvectors

of the global structure are recovered by $\bar{\boldsymbol{\Phi}} = \boldsymbol{\Phi}_{\mathrm{m}}^{\mathrm{p}} \mathbf{z}_{\mathrm{m}}$. $\varsigma = \boldsymbol{\Gamma}_{\mathrm{s}}^{\mathrm{T}} \left(\boldsymbol{\Lambda}_{\mathrm{s}}^{\mathrm{p}}\right)^{-1} \boldsymbol{\Gamma}_{\mathrm{s}}$ is associated with the first-order residual flexibility that can be calculated using the master modes of the substructures as

$$\boldsymbol{\Gamma}_{\mathrm{s}}^{\mathrm{T}} \left(\boldsymbol{\Lambda}_{\mathrm{s}}^{\mathrm{p}}\right)^{-1} \boldsymbol{\Gamma}_{\mathrm{s}} = \mathbf{C} \boldsymbol{\Phi}_{\mathrm{s}}^{\mathrm{p}} \left(\boldsymbol{\Lambda}_{\mathrm{s}}^{\mathrm{p}}\right)^{-1} \left[\boldsymbol{\Phi}_{\mathrm{s}}^{\mathrm{p}}\right]^{\mathrm{T}} \mathbf{C}^{\mathrm{T}} \tag{17}$$

$$\boldsymbol{\Phi}_{\mathrm{s}}^{\mathrm{p}} \left(\boldsymbol{\Lambda}_{\mathrm{s}}^{\mathrm{p}}\right)^{-1} \left[\boldsymbol{\Phi}_{\mathrm{s}}^{\mathrm{p}}\right]^{\mathrm{T}} = \begin{bmatrix} \left(\mathbf{K}^{(1)}\right)^{-1} - \boldsymbol{\Phi}_{\mathrm{m}}^{(1)} \left(\boldsymbol{\Lambda}_{\mathrm{m}}^{(1)}\right)^{-1} \left[\boldsymbol{\Phi}_{\mathrm{m}}^{(1)}\right]^{\mathrm{T}} & \mathbf{0} & \mathbf{0} \\ \mathbf{0} & \ddots & \mathbf{0} \\ \mathbf{0} & \mathbf{0} & \left(\mathbf{K}^{(N_S)}\right)^{-1} - \boldsymbol{\Phi}_{\mathrm{m}}^{(N_S)} \left(\boldsymbol{\Lambda}_{\mathrm{m}}^{(N_S)}\right)^{-1} \left[\boldsymbol{\Phi}_{\mathrm{m}}^{(N_S)}\right]^{\mathrm{T}} \end{bmatrix} \tag{18}$$

In the present substructuring method, the higher modes of the substructures are not calculated and are compensated with the first-order residual flexibility. In Eq. (13), the nonlinear item $\left(\boldsymbol{\Lambda}_{\mathrm{s}}^{\mathrm{p}} - \bar{\lambda}\mathbf{I}\right)^{-1}$ is approximately represented by the first item of Taylor expansion $\left(\boldsymbol{\Lambda}_{\mathrm{s}}^{\mathrm{p}}\right)^{-1}$, and the error introduced by this approximation is

$$\begin{aligned} \textit{Error} = \left(\boldsymbol{\Lambda}_{\mathrm{s}}^{\mathrm{p}} - \bar{\lambda}\mathbf{I}\right)^{-1} - \left(\boldsymbol{\Lambda}_{\mathrm{s}}^{\mathrm{p}}\right)^{-1} &= \begin{bmatrix} \dfrac{1}{\left(\boldsymbol{\Lambda}_{\mathrm{s}}^{\mathrm{p}}\right)_1 - \bar{\lambda}} - \dfrac{1}{\left(\boldsymbol{\Lambda}_{\mathrm{s}}^{\mathrm{p}}\right)_1} & & \\ & \ddots & \\ & & \dfrac{1}{\left(\boldsymbol{\Lambda}_{\mathrm{s}}^{\mathrm{p}}\right)_{NP_{\mathrm{s}}} - \bar{\lambda}} - \dfrac{1}{\left(\boldsymbol{\Lambda}_{\mathrm{s}}^{\mathrm{p}}\right)_{NP_{\mathrm{s}}}} \end{bmatrix} \\ &= \begin{bmatrix} \dfrac{\bar{\lambda}}{\left(\left(\boldsymbol{\Lambda}_{\mathrm{s}}^{\mathrm{p}}\right)_1 - \bar{\lambda}\right)\left(\boldsymbol{\Lambda}_{\mathrm{s}}^{\mathrm{p}}\right)_1} & & \\ & \ddots & \\ & & \dfrac{\bar{\lambda}}{\left(\left(\boldsymbol{\Lambda}_{\mathrm{s}}^{\mathrm{p}}\right)_{NP_{\mathrm{s}}} - \bar{\lambda}\right)\left(\boldsymbol{\Lambda}_{\mathrm{s}}^{\mathrm{p}}\right)_{NP_{\mathrm{s}}}} \end{bmatrix} = \mathrm{Diag}\left(\frac{\bar{\lambda}}{\left(\left(\boldsymbol{\Lambda}_{\mathrm{s}}^{\mathrm{p}}\right)_i - \bar{\lambda}\right)\left(\boldsymbol{\Lambda}_{\mathrm{s}}^{\mathrm{p}}\right)_i} \right) \end{aligned} \tag{19}$$

$$\textit{Relative error} = \mathrm{Diag}\left(\frac{\dfrac{\bar{\lambda}}{\left(\left(\boldsymbol{\Lambda}_{\mathrm{s}}^{\mathrm{p}}\right)_i - \bar{\lambda}\right)\left(\boldsymbol{\Lambda}_{\mathrm{s}}^{\mathrm{p}}\right)_i}}{\dfrac{1}{\left(\boldsymbol{\Lambda}_{\mathrm{s}}^{\mathrm{p}}\right)_i - \bar{\lambda}}} \right) = \mathrm{Diag}\left(\frac{\bar{\lambda}}{\left(\boldsymbol{\Lambda}_{\mathrm{s}}^{\mathrm{p}}\right)_i} \right) \qquad (i=1, 2, \ldots, NP_{\mathrm{s}}) \tag{20}$$

Therefore, the largest relative error = $\dfrac{\bar{\lambda}}{\min\left(\mathbf{\Lambda}_{\mathrm{s}}^{\mathrm{p}}\right)}$.

It reveals that the relative error of this substructuring method is dependent on $\dfrac{\bar{\lambda}}{\min\left(\mathbf{\Lambda}_{\mathrm{s}}^{\mathrm{p}}\right)}$. If the required eigenvalues $\bar{\lambda}$ are far less than the minimum value of $\mathbf{\Lambda}_{\mathrm{s}}^{\mathrm{p}}$, the introduced error will be insignificant. That is to say, the minimum value of $\mathbf{\Lambda}_{\mathrm{s}}^{\mathrm{p}}$ will control the accuracy of the proposed substructuring method. As $\mathbf{\Lambda}_{\mathrm{s}}^{\mathrm{p}}$ includes the eigenvalues of the slave modes of the substructures, retaining more master modes in the substructures can increase the values in $\mathbf{\Lambda}_{\mathrm{s}}^{\mathrm{p}}$. One should determine how many master modes need to be calculated in each substructure according to the precision required. The influence of this slight error on model updating results will be investigated through a numerical example in Section 5.

4. Eigensensitivity with substructuring method

The eigensensitivity of the *i*th mode (*i*=1, 2, …, *N*) with respect to an elemental parameter will be derived in this section. The elemental parameter is chosen to be the stiffness parameter, such as the bending rigidity of an element, and denoted as parameter *r* in the *R*th substructure. The reduced eigenequation (Eq. (16)) is rewritten for the *i*th mode as

$$\left[\left(\mathbf{\Lambda}_{\mathrm{m}}^{\mathrm{p}}-\bar{\lambda}_i\mathbf{I}_{\mathrm{m}}\right)+\mathbf{\Gamma}_{\mathrm{m}}\varsigma^{-1}\mathbf{\Gamma}_{\mathrm{m}}^{\mathrm{T}}\right]\{\mathbf{z}_i\}=\{\mathbf{0}\} \tag{21}$$

Eq. (21) is differentiated with respect to parameter *r* as

$$\left[\left(\boldsymbol{\Lambda}_{\mathrm{m}}^{\mathrm{p}}-\bar{\lambda}_i\mathbf{I}_{\mathrm{m}}\right)+\boldsymbol{\Gamma}_{\mathrm{m}}\varsigma^{-1}\boldsymbol{\Gamma}_{\mathrm{m}}^{\mathrm{T}}\right]\frac{\partial\{\mathbf{z}_i\}}{\partial r}+\frac{\partial\left[\left(\boldsymbol{\Lambda}_{\mathrm{m}}^{\mathrm{p}}-\bar{\lambda}_i\mathbf{I}_{\mathrm{m}}\right)+\boldsymbol{\Gamma}_{\mathrm{m}}\varsigma^{-1}\boldsymbol{\Gamma}_{\mathrm{m}}^{\mathrm{T}}\right]}{\partial r}\{\mathbf{z}_i\}=\{\mathbf{0}\} \tag{22}$$

Since $\left[\left(\boldsymbol{\Lambda}_{\mathrm{m}}^{\mathrm{p}}-\bar{\lambda}_i\mathbf{I}_{\mathrm{m}}\right)+\boldsymbol{\Gamma}_{\mathrm{m}}\varsigma^{-1}\boldsymbol{\Gamma}_{\mathrm{m}}^{\mathrm{T}}\right]$ is symmetric, pre-multiplying $\{\mathbf{z}_i\}^{\mathrm{T}}$ on both sides of Eq. (22) gives the eigenvalue derivative of the *i*th mode

$$\frac{\partial\bar{\lambda}_i}{\partial r}=\{\mathbf{z}_i\}^{\mathrm{T}}\left[\frac{\partial\boldsymbol{\Lambda}_{\mathrm{m}}^{\mathrm{p}}}{\partial r}+\frac{\partial\left(\boldsymbol{\Gamma}_{\mathrm{m}}\varsigma^{-1}\boldsymbol{\Gamma}_{\mathrm{m}}^{\mathrm{T}}\right)}{\partial r}\right]\{\mathbf{z}_i\} \tag{23}$$

where

$$\frac{\partial\left(\boldsymbol{\Gamma}_{\mathrm{m}}\varsigma^{-1}\boldsymbol{\Gamma}_{\mathrm{m}}^{\mathrm{T}}\right)}{\partial r}=\frac{\partial\boldsymbol{\Gamma}_{\mathrm{m}}}{\partial r}\varsigma^{-1}\boldsymbol{\Gamma}_{\mathrm{m}}^{\mathrm{T}}-\boldsymbol{\Gamma}_{\mathrm{m}}\varsigma^{-1}\frac{\partial\varsigma}{\partial r}\varsigma^{-1}\boldsymbol{\Gamma}_{\mathrm{m}}^{\mathrm{T}}+\boldsymbol{\Gamma}_{\mathrm{m}}\varsigma^{-1}\frac{\partial\boldsymbol{\Gamma}_{\mathrm{m}}^{\mathrm{T}}}{\partial r} \tag{24}$$

In this equation, the derivative matrices $\frac{\partial\boldsymbol{\Lambda}_{\mathrm{m}}^{\mathrm{p}}}{\partial r}$, $\frac{\partial\boldsymbol{\Gamma}_{\mathrm{m}}}{\partial r}$, and $\frac{\partial\varsigma}{\partial r}$ are formed using the eigenvalue derivatives, eigenvector derivatives, and residual flexibility derivatives of the substructures. Since the substructures are independent, these derivative matrices are calculated within the *R*th substructure solely, while those in other substructures are zeros, i.e.,

$$\frac{\partial\boldsymbol{\Lambda}_{\mathrm{m}}^{\mathrm{p}}}{\partial r}=\begin{bmatrix}\mathbf{0}&\mathbf{0}&\mathbf{0}\\ \mathbf{0}&\frac{\partial\boldsymbol{\Lambda}_{\mathrm{m}}^{(R)}}{\partial r}&\mathbf{0}\\ \mathbf{0}&\mathbf{0}&\mathbf{0}\end{bmatrix},\quad \frac{\partial\boldsymbol{\Gamma}_{\mathrm{m}}^{\mathrm{T}}}{\partial r}=\mathbf{C}\frac{\partial\boldsymbol{\Phi}_{\mathrm{m}}^{\mathrm{p}}}{\partial r}=\mathbf{C}\begin{bmatrix}\mathbf{0}&\mathbf{0}&\mathbf{0}\\ \mathbf{0}&\frac{\partial\boldsymbol{\Phi}_{\mathrm{m}}^{(R)}}{\partial r}&\mathbf{0}\\ \mathbf{0}&\mathbf{0}&\mathbf{0}\end{bmatrix}$$

$$\frac{\partial\varsigma}{\partial r}=\mathrm{C}\times\mathrm{Diag}\begin{bmatrix}\mathbf{0}&\mathbf{0}&\mathbf{0}\\ \mathbf{0}&\frac{\partial\left(\left(\mathbf{K}^{(R)}\right)^{-1}-\boldsymbol{\Phi}_{\mathrm{m}}^{(R)}\left(\boldsymbol{\Lambda}_{\mathrm{m}}^{(R)}\right)^{-1}\left[\boldsymbol{\Phi}_{\mathrm{m}}^{(R)}\right]^{\mathrm{T}}\right)}{\partial r}&\mathbf{0}\\ \mathbf{0}&\mathbf{0}&\mathbf{0}\end{bmatrix}\times\mathrm{C}^{\mathrm{T}} \tag{25}$$

$\{\mathbf{z}_i\}$, $\boldsymbol{\Gamma}_{\mathrm{m}}$, and ς^{-1} have been computed in previous section for eigensolutions and can be re-used here directly. $\frac{\partial\boldsymbol{\Lambda}_{\mathrm{m}}^{(R)}}{\partial r}$ and $\frac{\partial\boldsymbol{\Phi}_{\mathrm{m}}^{(R)}}{\partial r}$ are the eigensolution derivatives of the master modes in the *R*th substructures. They can be calculated with common methods, such as Nelson's method [19], by

treating the *R*th substructure as one independent structure. Subsequently, the eigenvalue derivative of the global structure can be obtained from Eq. (21), and it solely relies on a particular substructure (the *R*th substructure).

Regarding Eq. (16), the eigenvectors of the global structure are recovered by $\bar{\boldsymbol{\Phi}} = \boldsymbol{\Phi}_{\mathrm{m}}^{\mathrm{p}} \mathbf{z}_{\mathrm{m}}$. Hence, the *i*th eigenvector of the global structure can be expressed as

$$\bar{\boldsymbol{\Phi}}_i = \boldsymbol{\Phi}_{\mathrm{m}}^{\mathrm{p}} \{\mathbf{z}_i\} \tag{26}$$

Differentiating Eq. (26) with respect to the elemental parameter *r*, one can obtain the eigenvector derivative of the *i*th mode as

$$\frac{\partial \bar{\boldsymbol{\Phi}}_i}{\partial r} = \frac{\partial \boldsymbol{\Phi}_{\mathrm{m}}^{\mathrm{p}}}{\partial r} \{\mathbf{z}_i\} + \boldsymbol{\Phi}_{\mathrm{m}}^{\mathrm{p}} \left\{\frac{\partial \mathbf{z}_i}{\partial r}\right\} \tag{27}$$

In Eq. (27), $\boldsymbol{\Phi}_{\mathrm{m}}^{\mathrm{p}}$ and $\{\mathbf{z}_i\}$ have been obtained when calculating the eigensolutions. $\frac{\partial \boldsymbol{\Phi}_{\mathrm{m}}^{\mathrm{p}}}{\partial r}$ is associated with the eigenvector derivatives of the *R*th substructure as Eq. (25). $\left\{\frac{\partial \mathbf{z}_i}{\partial r}\right\}$ can be obtained from the reduced eigenequation (Eq. (21)), as described in the following.

$\left\{\frac{\partial \mathbf{z}_i}{\partial r}\right\}$ is separated into the sum of a particular part and a homogeneous part as

$$\left\{\frac{\partial \mathbf{z}_i}{\partial r}\right\} = \{v_i\} + c_i \{\mathbf{z}_i\} \tag{28}$$

where c_i is a participation factor. Substituting Eq. (28) into Eq. (22) gives:

$$\boldsymbol{\Psi} \{v_i\} = \{Y_i\} \tag{29}$$

where

$$\mathbf{\Psi}=\left[\left(\mathbf{\Lambda}_{\mathrm{m}}^{\mathrm{p}}-\bar{\lambda}_i\mathbf{I}_{\mathrm{m}}\right)+\mathbf{\Gamma}_{\mathrm{m}}\varsigma^{-1}\mathbf{\Gamma}_{\mathrm{m}}^{\mathrm{T}}\right],\quad \{Y_i\}=-\frac{\partial\left[\left(\mathbf{\Lambda}_{\mathrm{m}}^{\mathrm{p}}-\bar{\lambda}_i\mathbf{I}_{\mathrm{m}}\right)+\mathbf{\Gamma}_{\mathrm{m}}\varsigma^{-1}\mathbf{\Gamma}_{\mathrm{m}}^{\mathrm{T}}\right]}{\partial r}\{\mathbf{z}_i\}$$

Since the items in $\mathbf{\Psi}$ and $\{Y_i\}$ are available when calculating the eigenvalue derivatives, the vector $\{v_i\}$ can be solved with Eq. (29) effortlessly.

The eigenvector $\{\mathbf{z}_i\}$ of the reduced eigenequation (Eq. (16)) satisfies the orthogonal condition of

$$\{\mathbf{z}_i\}^{\mathrm{T}}\{\mathbf{z}_i\}=1 \tag{30}$$

Differentiating Eq. (30) with respect to r gives

$$\frac{\partial\{\mathbf{z}_i\}^{\mathrm{T}}}{\partial r}\{\mathbf{z}_i\}+\{\mathbf{z}_i\}^{\mathrm{T}}\frac{\partial\{\mathbf{z}_i\}}{\partial r}=0 \tag{31}$$

Substituting Eq. (28) into Eq. (31), the participation factor c_i is therefore obtained as

$$c_i=-\frac{1}{2}\left(\{v_i\}^{\mathrm{T}}\{\mathbf{z}_i\}+\{\mathbf{z}_i\}^{\mathrm{T}}\{v_i\}\right) \tag{32}$$

Given the vector $\{v_i\}$ and the participation factor c_i, the first-order derivative of $\{\mathbf{z}_i\}$ with respect to the elemental parameter r can be achieved as

$$\left\{\frac{\partial\mathbf{z}_i}{\partial r}\right\}=\{v_i\}-\frac{1}{2}\left(\{v_i\}^{\mathrm{T}}\{\mathbf{z}_i\}+\{\mathbf{z}_i\}^{\mathrm{T}}\{v_i\}\right)\{\mathbf{z}_i\} \tag{33}$$

Finally, the eigenvector derivative of the global structure can be calculated using Eq. (27), based on the items $\left\{\frac{\partial\mathbf{z}_i}{\partial r}\right\}$, $\frac{\partial\mathbf{\Phi}_{\mathrm{m}}^{\mathrm{p}}}{\partial r}$, $\mathbf{z}_i$ and $\mathbf{\Phi}_{\mathrm{m}}^{\mathrm{p}}$.

Since the reduced eigenequation (Eq. (21)) is smaller in size compared to that of the global structure (Eq. (5)), calculation of $\left\{\frac{\partial\mathbf{z}_i}{\partial r}\right\}$ can be processed much faster than that in the conventional Nelson's

method based on the global eigenequation (Eq. (5)). As calculation of the eigenvector derivatives dominates the whole model updating process, the substructuring method will improve the computational efficiency significantly, as demonstrated in the following examples.

5. Numerical example: a frame structure

As explained previously, the contribution of the slave modes to the eigenequation of the global structure are approximately compensated by the first-order residual flexibility matrix. This introduces some slight errors in calculation of the eigensolutions and eigensensitivities, and is regarded as methodology error [24]. A simulated frame structure (Fig. 1) is first employed to investigate the influence of this methodology error on model updating results. The frame structure comprises 160 two-dimensional beam elements as labeled in Fig. 1(a). There are 140 nodes and 408 DOFs in total. The material constants of the beam elements are chosen as: bending rigidity (EI) $=170\times 10^6$ Nm^2, axial rigidity (EA) = 2500×10^6 N, mass per unit length (ρA) = 110 kg/m, and Poisson's ratio = 0.3.

In model updating, the simulated “experimental” modal data are usually obtained by intentionally introducing damages on some elements, and then the analytical model is updated to identify these damages [1, 6, 25]. In the present paper, the simulated frequencies and mode shapes, which are treated as the “experimental” data, are calculated from the FE model by intentionally reducing the

bending rigidity of some elements [25]. The simulated reduction in bending rigidity is listed in Table 1 and denoted in Fig. 1(a). The first 10 “experimental” modes are available, and the measurements are obtained at the points and directions denoted in Fig. 1(a). Both the “experimental” frequencies and mode shapes are utilized to update the analytical model. The mode shapes have been normalized with respect to the mass matrix.

The eigensolutions and eigensensitivities of the analytical model are calculated using the proposed substructuring method, and match the “experimental” counterparts through an optimization process. Using the substructuring method, the frame is disassembled into three substructures (N_S = 3) when torn at 8 nodes as Fig. 1(b). The first 30 modes are retained as master modes in each substructure to calculate the first 10 eigensolutions and eigensensitivities of the global structure. It is noted that using the proposed substructuring method, the eigensolutions and eigensensitivities are calculated based on the reduced equation (Eq. (16)) with size of 90×90, rather than on the original global eigenequation (Eq. (5)) with size of 408×408. The eigenmodes and eigensensitivities at the experimentally measured points are then singled out to match the “experimental” modal data for model updating purpose. The bending rigidity of all column elements is assumed as unknown and chosen as the updating parameter. Accordingly, there are 64 updating parameters in total.

The optimization is processed with the trust-region method provided by the Matlab Optimization

Toolbox [17, 26]. The algorithm can automatically select the steps and searching directions according to the objective function (discrepancy of eigensolutions) and the provided eigensensitivity matrices. The model updating process stops when the pre-defined tolerance of the objective function (Eq. (1)) or the maximum number of the iterations is reached.

The influence of the methodology error on model updating results is first investigated by simulating the "experimental" data without introducing any discrepancy on the elemental parameters, as the 1st case (Table 1). The analytical eigensolutions are calculated using the substructuring method, and compared with the "experimental" data in Table 2. Some minor differences are found in Table 2, as expected. The relative differences in frequencies are less than 0.3% for all modes. The MAC values [27], which indicate the similarity of the analytical and experimental mode shapes, are above 0.99. This verifies that the error of the proposed substructuring method in calculation of eigensolutions is very small. Model updating is conducted to find out the change of the elemental bending rigidity due to the slight errors in calculation of eigensolutions and eigensensitivity. Fig. 2(a) gives the proportional changes in the elemental bending rigidity before and after updating that are calculated using the proposed substructure-based model updating method. The small values observed in Fig. 2(a) demonstrate that the slight errors in calculation of the eigensolutions and eigensensitivities have negligible effects on the model updating results. The errors come from the approximation of the higher modes with the residual flexibility matrix, as quantified in Eq. (19) and Eq. (20),

The “experimental” modal data is then generated by introducing certain known discrepancies in the bending rigidity of some elements, which are given in Table 1. In the 2nd case, the bending rigidity of a randomly selected column in the 1st substructure is assumed to be reduced by 30%. The column is composed of Element 147 and Element 148, denoted by ‘D1’ in Fig. 1(a). That is, the bending rigidity of Element 147 and Element 148 are reduced by 30% while the other elements remain unchanged. All the elements are then reassembled into a structure to obtain the “experimental” frequencies and mode shapes. The model updating process is conducted to make the analytical model reproduce the “experimental” frequencies and mode shapes. The frequencies and mode shapes before and after the updating are compared in Table 3. It demonstrates that the analytical modal data closely match the simulated “experimental” counterparts after the updating. The identified changes of the elemental parameters are illustrated in Fig. 2(b). The stiffness parameters of Element 147 and Element 148 are reduced by 30%, which agree with the simulated reduction in the elemental parameters. Some small values observed in other elements are due to the errors in calculation of eigensolutions and eigensensitivity, which have negligible influence on the model updating results.

Without losing generality, the bending rigidity of elements located in different substructures are assumed to have some known discrepancy as well. In the 3rd case, the bending rigidity of two columns (denoted by ‘D1’ and ‘D2’ in Fig. 1(a)) is assumed to be reduced by 30% and 20% (see Table 1), respectively, i.e., the bending rigidity of Elements 147 and 148 are reduced by 30% and the

bending rigidity of Elements 139 and 140 are reduced by 20%. All the elements are then assembled into a model to generate the 'experimental' frequencies and mode shapes. The proposed substructure-based model updating method is used to adjust the elemental parameters of the analytical model, to match the simulated "experimental" modes. The frequencies and mode shapes before and after the updating are compared with the "experimental" ones in Table 4, and the identified variation of bending rigidity is shown in Fig. 2(c). In Table 4, the frequencies and mode shapes of the updated model better match the "experimental" counterparts, as compared with those before updating. In Fig. 2(c), obvious negative values are observed in Elements 139, 140, 147 and 148. In particular, the bending rigidity of Elements 138 and 140 are identified to be reduced by about 0.2 and those of Elements 147 and 148 are reduced by about 0.3. The location and severity of the identified reduction in elemental parameters agree with the simulated ones very well.

Case 2 and Case 3 verify that the location and severity of the assumed reduction in elemental stiffness can be successfully identified through the proposed substructure-based model updating method. It again proves that the influence of the methodology errors is insignificant, when proper size of the master modes is retained. One can improve the accuracy of the eigensolutions and eigensensitivities by including more master modes in the substructures [15, 16]. The proposed substructuring method is effective to be applied in model updating process.

6. Practical application: a bridge structure

To illustrate the feasibility and computational efficiency of the proposed substructuring method in real structures, a practical bridge, the Balla Balla River Bridge in Western Australia is employed here. An FE model based on design drawings was established. The FE model of this bridge has 907 elements, 947 nodes each has 6 DOFs, and 5420 DOFs in total, as shown in Fig. 3.

In the field vibration testing, the accelerometers were placed in seven rows corresponding to the seven girders. There are 19 measurement points in each row and 133 in total as shown in Fig. 4. Ten pairs of natural frequencies and mode shapes were extracted from the frequency response function (FRF) by the rational fraction polynomial method [28], and some of them are illustrated in Fig.5.

The analytical model is updated employing both the traditional model updating procedure and the proposed substructure-based model updating method for comparison. There are 1289 physical parameters selected as updating candidates, which include the Young's modulus (E) of diaphragms, girders, slabs, and the axial stiffness (EA) and bending rigidity (EI_{xx}, EI_{yy}) of the shear connectors. The objective function combines the differences in the frequencies and mode shapes between the experimental test and analytical model. The weight coefficients are set to 0.1 for the mode shapes and 1.0 for the frequencies.

Using the traditional model updating method, the eigensolutions and eigensensitivities are calculated based on the system matrices of the global structure [29]. The Lanczos method is employed to calculate the eigensolutions and the Nelson's method is used for the eigensensitivities [19, 21]. In each iteration, the first 30 eigenmodes are calculated from the FE model to compare with the 10 modes measured in field testing. The model updating process is terminated after 69 iterations, which costs 86.16 hours on an ordinary personal computer. One iteration takes about 1.26 hours. The convergence process in terms of the norm of the objective function is demonstrated in Fig. 6.

Using the proposed substructuring method, the eigensolutions and eigensensitivities of the global structure are calculated in substructure manner in each iteration. The optimization algorithm, updating parameters, and convergence criterion are the same as those used in the previous traditional model updating. The global structure is divided into 11 substructures along the longitudinal direction as shown in Fig. 3. The detailed information of the 11 substructures is listed in Table 5. In each iteration, a few eigensolutions of the independent substructures are calculated to obtain the eigensolutions of the global structure. To calculate the eigensensitivity of the global structure with respect to an elemental parameter, the derivative matrices of only one substructure that contains the elements is required while those in other substructures are set to zero.

As stated previously, the number of the master modes retained in the substructures influences the

accuracy of the eigensolutions and eigensensitivities, and subsequently, affects the convergence of the model updating process. In model updating process, more accurate eigensolutions and eigensensitivities are required when the results are close to the optimum, as some errors in eigensolutions and eigensensitivities may lead to an incorrect search direction and thus cause the convergence difficulties. In the present paper, different number of master modes is employed in the substructures according to the progress of the model updating procedure. In the beginning, the first 40 modes of each substructure were retained as master modes to calculate the first 30 eigensolutions and eigensensitivities of the global structure. The number of master modes in the substructures was then enlarged gradually as the convergence slowed down. At the final steps, 90 modes were retained in each substructure to improve the accuracy of the eigensolutions and eigensensitivities. With this adaptive scheme, the substructure-based model updating process is completed within 76 iterations and the convergence process is demonstrated in Fig. 4. The computation time spent on different stages is listed in Table 6 and totals about 48.07 hours, which is about 56% of that using the traditional global model updating method.

The frequencies and mode shapes of the updated structure are compared with those values before updating as listed in Table 7. It is observed that the proposed substructuring method can achieve similar results to the global method. In particular, the averaged difference in frequencies between the updated model and the experimental measurement is less than 1%. The MAC values are improved

from 0.85 to 0.93. As compared with the traditional model updating method, this substructure-based model updating method achieves the same precision but higher efficiency.

7. Conclusion

This paper has proposed a substructuring method to calculate the eigensolutions and eigensensitivities for the model updating purposes. The eigensolutions of the global structure are calculated from some lowest modes of the substructures. Calculation of the eigensensitivities with respect to an elemental parameter requires analysis of the sole substructure that contains the element. Since the model updating process involves frequent calculation of the eigensolutions and eigensensitivities, this substructure-based model updating method is advantageous in improving the computational efficiency.

The effectiveness of the substructure-based model updating method was illustrated by a frame structure. Although the substructuring method introduces some slight errors in calculation of the eigensolutions and eigensensitivities, the effect of the errors on the model updating results is negligible when proper master modes are retained in the substructures. Application to a practical bridge demonstrates that the proposed substructure-based model updating is efficient to be applied to update large-scale structures with a large number of design parameters. The accuracy of the proposed substructuring method is improved by including more master modes in the substructures.

Acknowledgements

The work described in this paper is supported by a grant from the Research Grants Council of the Hong Kong Special Administrative Region, China (Project No. PolyU 5321/08E). The first author is grateful to the Department of Civil and Structural Engineering, the Hong Kong Polytechnic University for the scholarship provided.

References

[1] Mottershead JE, Friswell MI. Model updating in structural dynamics: A survey. Journal of Sound and Vibration 1993; **167**: 347-75.

[2] Brownjohn JMW, Xia PQ. Dynamic assessment of curved cable-stayed bridge by model updating. Journal of structural engineering 2000; **126**: 252-60.

[3] Brownjohn JMW, Moyo P, Omenzetter P, Lu Y. Assessment of Highway Bridge Upgrading by Dynamic Testing and Finite-Element Model Updating. Journal of Bridge Engineering 2003; **8**: 162-72.

[4] Jaishi B, Ren WX. Structural Finite Element Model Updating Using Ambient Vibration Test Results. Journal of Structural Engineering 2005; **131**: 617-28.

[5] Zivanovic S, Pavic A, Reynolds P. Finite element modeling and updating of a lively footbridge:

The complete process. Journal of Sound and Vibration 2007; **301**: 126-45.

[6] Brownjohn JMW, Xia PQ, Hao H, Xia Y. Civil structure condition assessment by FE model updating: methodology and case studies. Finite Elements in Analysis and Design 2001; **37**: 761-75.

[7] Bakira PG, Reynders E, Roeck GD. Sensitivity-based finite element model updating using constrained optimization with a trust region algorithm. Journal of Sound and Vibration 2007; **305**: 211-25.

[8] Craig RR. Coupling of substructures for dynamic analyses: An overview. In AIAA/ASME/ASCE/AHS/ASC 41st Structures, Structural Dynamics, and Materials Conference, Atlanta, GA, 2000. p. 3-17.

[9] Klerk D, Rixen DJ, Voormeeren SN. General Framework for Dynamic Substructuring: History, Review, and Classification of Techniques. AIAA Journal 2008; **46**: 1169-81.

[10] Perera R, Ruiz A. A multistage FE updating procedure for damage identification in large-scale structures based on multiobjective evolutionary optimization. Mechanical Systems and Signal Processing 2008; 22: 970-91.

[11] Ko JM, Sun ZG, Ni YQ. Multi-stage identification scheme for detecting damage in cable-stayed Kap Shui Mun Bridge. Engineering Structures 2002; 24: 857-68.

[12] Xia Y, Lin RM. Improvement on the iterated IRS method for structural eigensolutions. Journal of Sound and Vibration 2004; **270**: 713-27.

[13] Xia Y, Lin RM. A new iterative order reduction (IOR) method for eigensolutions of large structures. International Journal for Numerical Method in Engineering 2004; **59**: 153-72.

[14] Kron G. Diakoptics. London: Macdonald and Co.; 1963.

[15] Weng S, Xia Y, Xu YL, Zhou XQ, Zhu HP. Improved substructuring method for eigensolutions of large-scale structures. Journal of Sound and Vibration 2009; **323**: 718-36

[16] Xia Y, Weng S, Xu YL. A substructuring method for calculation of eigenvalue derivatives and eigenvector derivatives. The 4th International Conference on Structural Health Monitoring of Intelligent Infrastructure, 22-24 July, Zurich, Switzerland, 2009.

[17] Choi KK, Kim NH. Structural Sensitivity Analysis and Optimization 1: Linear Systems. New York: Springer Science and Business Media, Inc.; 2005.

[18] Fox RL, Kapoor MP. Rate of change of eigenvalues and eigenvectors. AIAA Journal 1968; **6**: 2426-9.

[19] Nelson RB. Simplified calculation of eigenvector derivatives. AIAA Journal 1976; **14**: 1201-5.

[20] Sutter TR, Camarda CJ, Walsh JL, Adelman WM. A comparison of several methods for the calculation of vibration mode shape derivatives. AIAA Journal 1988; **26**: 1506-11.

[21] Bathe KJ. Finite element procedures in engineering analysis. New Jersey: Prentice-hall, INC. Englewood chiffs; 1982.

[22] Sehmi NS. Large order structural eigenanalysis techniques algorithms for finite element systems. England: Ellis Horwood Limited, Chichester; 1989.

[23] Simpson A, Tabarrok B. On Kron's eigenvalue procedure and related methods of frequency analysis. Quarterly Journal of Mechanics and Applied Mathematics 1968; **21**: 1039-48.

[24] Xia Y. Condition Assessment of Structures Using Dynamic Data. Ph.D thesis. Nanyang Technological University, Singapore; 2002.

[25] Modak SV, Kundra TK, Nakra BC. Comparative study of model updating methods using simulated experimental data. Computers and Structures 2002; **80**: 437-47.

[26] Ewins DJ. Modal testing - theory, practice and application. Baldock: Research Studies Press Ltd; 2000.

[27] Zhang ZY. MATLAB: The Language of Technical Computing, Version 6.1. Beijing: Beihang University Press; 2003.

[28] Formenti DL, Richardson MH. Parameter estimation from frequency response measurements using rational fraction polynomials. The 20th International Modal Analysis Conference. Los Angeles, CA, 2002. p. 1-10.

[29] Xia Y, Hao H, Deeks AJ, Zhu XQ. Condition assessment of shear connectors in slab-girder bridges via vibration measurements. Journal of Bridge Engineering 2008; **13**: 43-54.

List of Figures

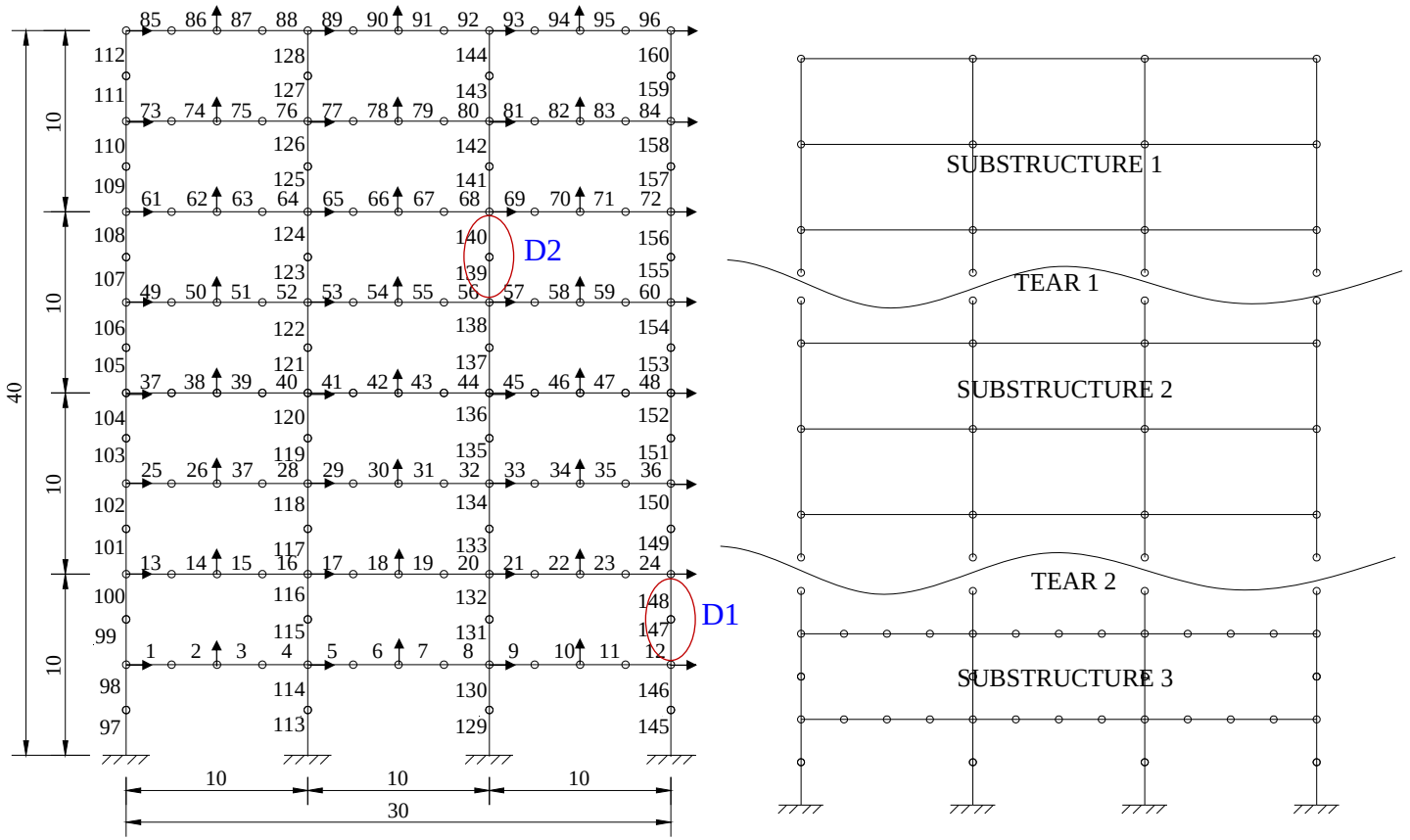

(a) The global structure (b) The divided substructures

Fig. 1. The frame structure.

→: the points and directions of experimental measurement.

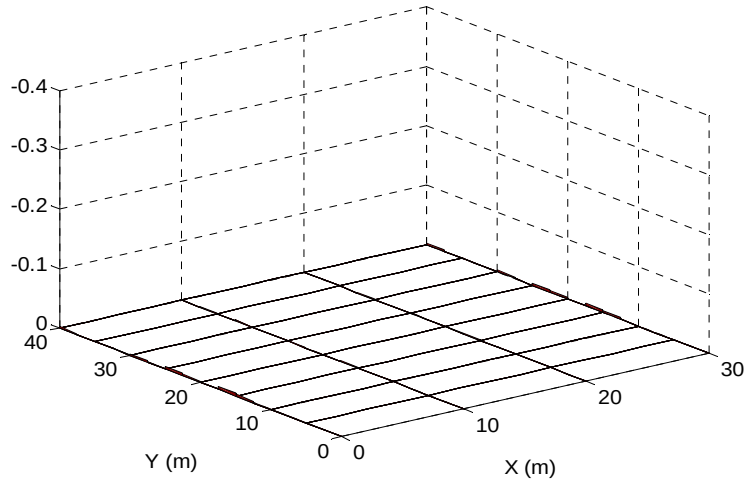

(a) Case 1

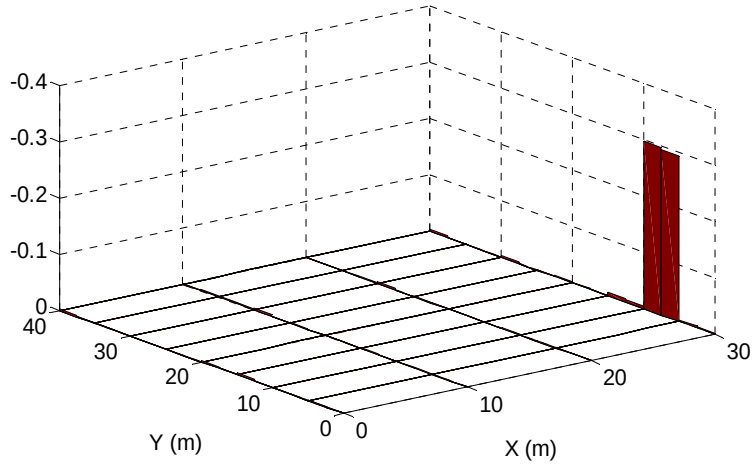

(a) Case 2

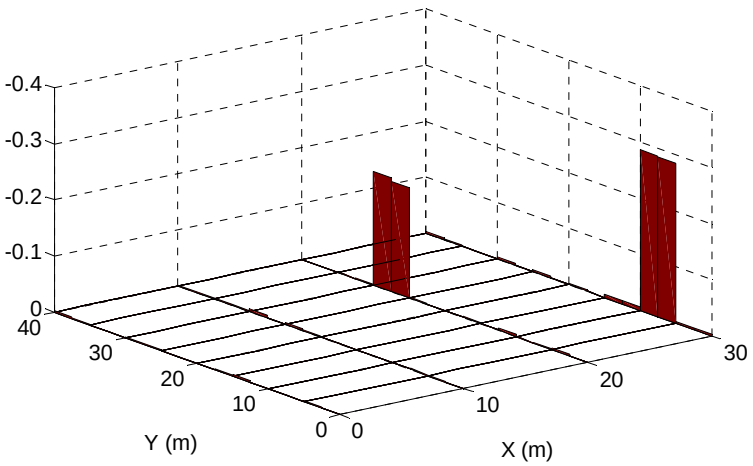

(a) Case 3

Fig. 2. Location and severity of discrepancies identified using the substructuring method.

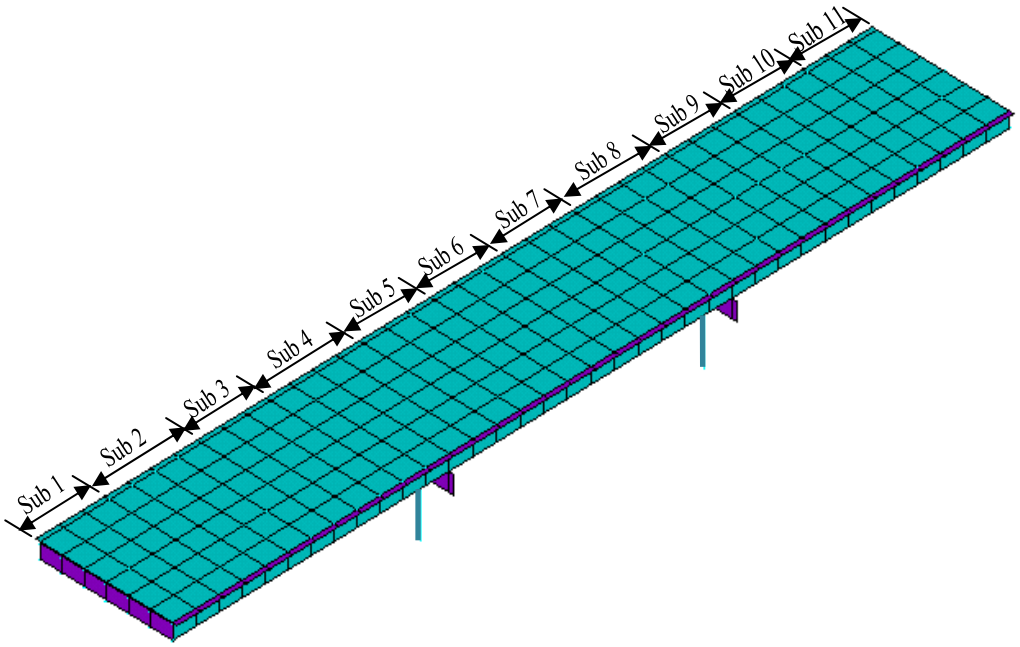

Fig. 3. The FE model of Balla Balla River Bridge with division formation of 11 substructures.

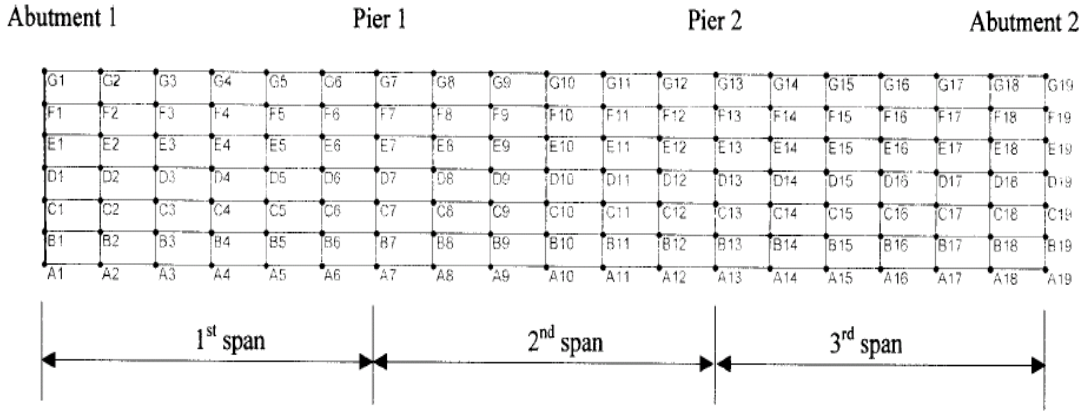

Fig. 4. Locations of sensors.

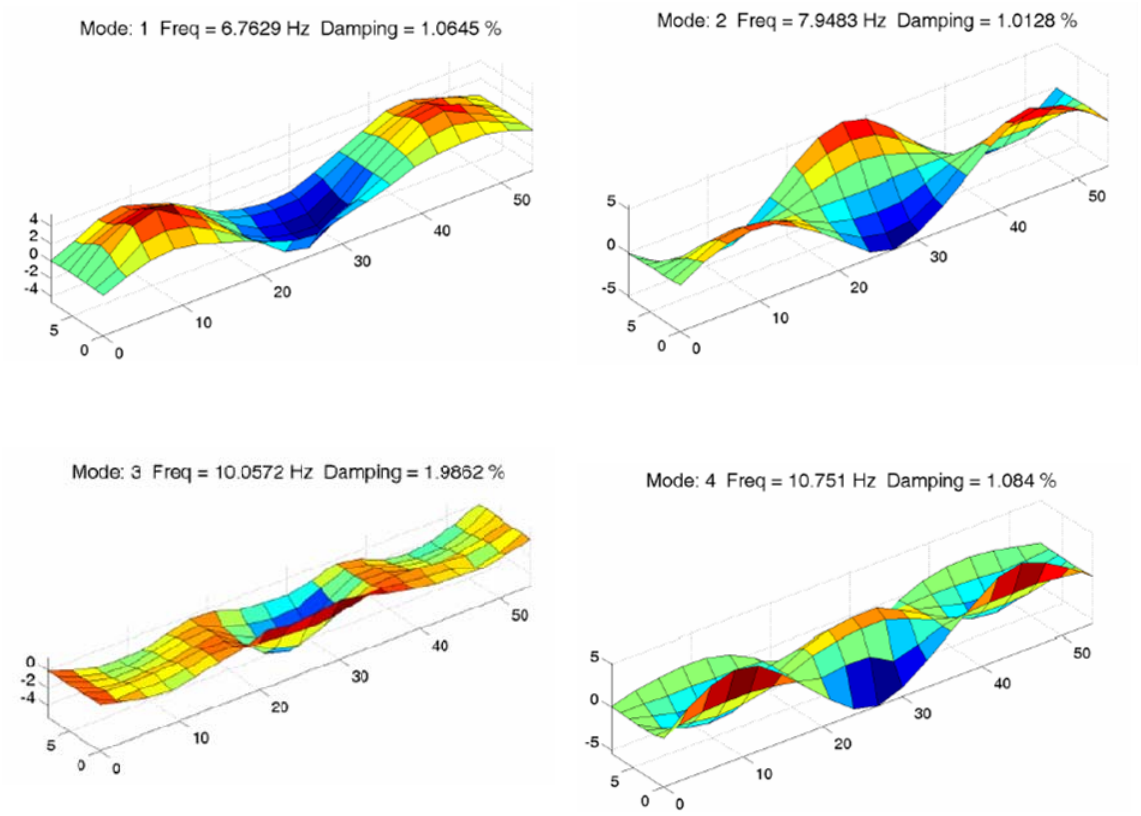

Fig.5. Measured frequencies and mode shapes of the Balla Balla River Bridge.

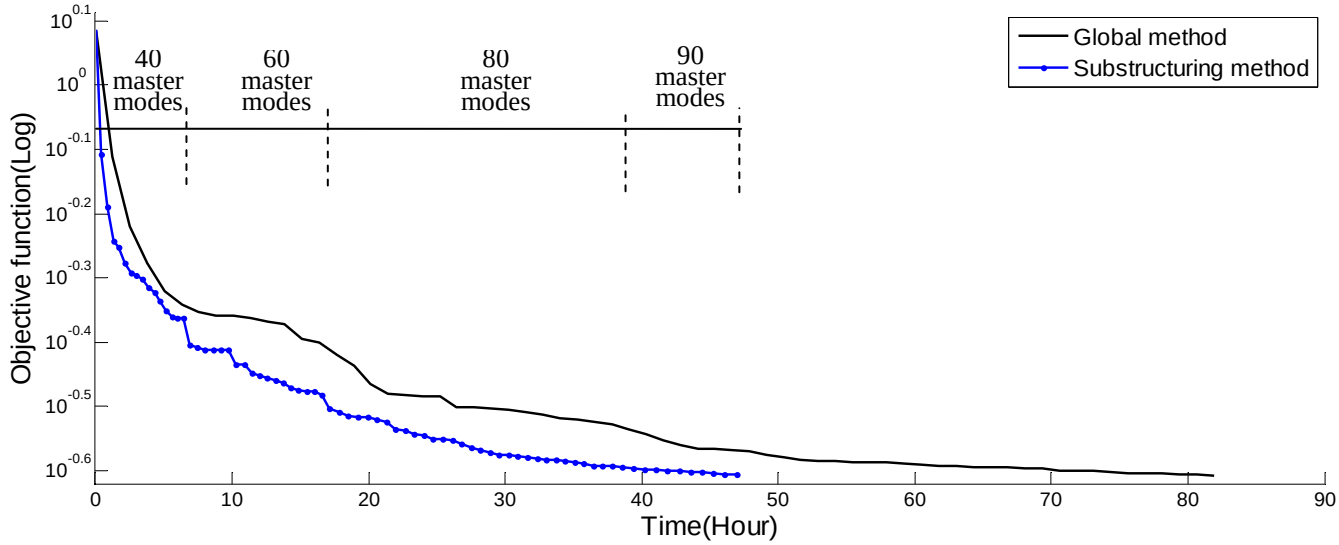

Fig. 6. The convergence of model updating with the substructuring method and the global method.

List of Tables

Table 1.
The assumed stiffness reduction in the elements.

	Case 1	Case 1	Case 2
Assumed discrepancy of bending rigidity	No discrepancy	Element 147(-30%); Element 148(-30%);	Element 147(-30%); Element 148(-30%); Element 139(-20%); Element 140(-20%);

Table 2.
The frequencies and mode shapes of the frame using the proposed substructuring method.

Modes	Experimental frequencies (Hz)	Analytical frequencies (Hz)	Difference (%)[a]	MAC[b]
1	2.1406	2.1406	0.000%	1.0000
2	6.6401	6.6401	0.000%	1.0000
3	11.7694	11.7695	0.001%	0.9999
4	17.5859	17.5862	0.002%	0.9999
5	19.5540	19.5891	0.179%	0.9967
6	22.1608	22.2017	0.184%	0.9958
7	24.1594	24.1601	0.003%	0.9999
8	26.7532	26.8147	0.230%	0.9949
9	30.3360	30.4001	0.211%	0.9941
10	31.2727	31.2801	0.024%	0.9986

[a] relative difference of frequency between the simulated experimental data and those predicted with the proposed substructuring method.
[b] modal assurance criterion (MAC) of mode shapes between the simulated experimental data and those predicted with the proposed substructuring method.

Table 3.
The frequencies and mode shapes of the frame structure before and after updating (case 2).

Modes	Experimental frequencies (Hz)	Before updating			After updating		
		Analytical frequencies (Hz)	Difference (%)[a]	MAC [b]	Analytical frequencies (Hz)	Difference (%)[a]	MAC [b]
1	2.1354	2.1406	0.241%	1.0000	2.1350	0.014%	1.0000
2	6.6279	6.6401	0.184%	1.0000	6.6266	0.019%	1.0000
3	11.7522	11.7695	0.147%	0.9999	11.7462	0.051%	1.0000
4	17.5502	17.5862	0.205%	0.9998	17.5495	0.004%	1.0000
5	19.4946	19.5891	0.485%	0.9934	19.4886	0.031%	1.0000
6	21.9613	22.2017	1.095%	0.9897	21.9541	0.032%	1.0000
7	24.0944	24.1601	0.272%	0.9995	24.0927	0.009%	1.0000
8	26.3567	26.8147	1.738%	0.9838	26.3537	0.012%	1.0000
9	30.0544	30.4101	1.183%	0.9791	30.0518	0.009%	0.9999
10	31.1147	31.2801	0.532%	0.9934	31.1048	0.031%	1.0000

[a] relative difference of frequency between the simulated experimental data and the model prediction.
[b] modal assurance criterion (MAC) of mode shapes between the simulated experimental data and the model prediction.

Table 4.
The frequencies and mode shapes of the frame structure before and after updating (case 3).

Modes	Experimental frequencies (Hz)	Before updating			After updating		
		Analytical frequencies (Hz)	Difference (%)[a]	MAC[b]	Analytical frequencies (Hz)	Difference (%)[a]	MAC[b]
1	2.1334	2.1406	0.337%	1.0000	2.1330	0.018%	1.0000
2	6.6070	6.6401	0.501%	1.0000	6.6057	0.020%	1.0000
3	11.7427	11.7695	0.228%	0.9998	11.7375	0.044%	1.0000
4	17.5042	17.5862	0.468%	0.9997	17.4970	0.041%	1.0000
5	19.4323	19.5891	0.807%	0.9927	19.4254	0.036%	1.0000
6	21.9215	22.2017	1.278%	0.9875	21.9138	0.035%	1.0000
7	24.0036	24.1601	0.652%	0.9987	23.9939	0.040%	1.0000
8	26.3274	26.8147	1.851%	0.9816	26.3236	0.014%	1.0000
9	30.0210	30.4101	1.296%	0.9775	29.9969	0.080%	0.9999
10	31.0952	31.2801	0.595%	0.9936	31.0866	0.027%	0.9999

[a] relative difference of frequency between the simulated experimental data and the model prediction.
[b] modal assurance criterion (MAC) of mode shapes between the simulated experimental data and the model prediction.

Table 5.
The information of division formation with 11 substructures.

Index of Substructure	Sub 1	Sub 2	Sub 3	Sub 4	Sub 5	Sub 6	Sub 7	Sub 8	Sub 9	Sub 10	Sub 11
Geometric range (m)	0~5	5~10	10~15	15~20	20~25	25~30	30~35	35~40	40~45	45~50	50~54
No. elements	99	88	66	116	66	66	66	116	66	66	99
No. nodes	113	115	92	143	92	92	92	143	92	92	113
No. tear nodes	23	23	23	23	23	23	23	23	23	23	

Table 6.
Comparison of the computation time and the number of iterations.

	Global method	Substructuring method			
		40 master modes	60 master modes	80 master modes	90 master modes
Time for each iteration (Hour)	1.26	0.43	0.57	0.69	0.84
No. of iterations	69	16	18	31	11
Total for the updating process (Hour)	86.16	48.07			

Table 7.
The frequencies and mode shapes of the bridge before and after updating.

Mode	Measured Frequency (Hz)	Before updating			After updating					
					Global method			Substructuring method		
		Frequency (Hz)	Difference (%)[a]	MAC[b]	Frequency (Hz)	Difference (%)[a]	MAC[b]	Frequency (Hz)	Difference (%)[a]	MAC[b]
1	6.76	6.26	7.34%	0.93	6.53	3.47%	0.95	6.55	3.17%	0.95
2	7.95	7.74	0.27%	0.96	7.93	0.27%	0.99	7.92	0.33%	0.99
3	10.06	8.71	13.37%	0.71	10.02	0.42%	0.94	10.02	0.39%	0.94
4	10.75	12.13	12.84%	0.80	11.01	2.42%	0.89	11.03	2.60%	0.89
5	11.03	9.45	14.36%	0.76	10.86	1.56%	0.82	10.85	1.60%	0.81
6	12.64	13.27	4.98%	0.85	12.58	0.45%	0.97	12.59	0.38%	0.96
7	14.71	17.55	19.29%	0.92	14.77	0.38%	0.90	14.78	0.45%	0.90
8	15.76	18.52	17.49%	0.88	15.77	0.03%	0.93	15.77	0.06%	0.94
9	16.39	18.74	14.35%	0.82	16.38	0.07%	0.95	16.39	0.00%	0.95
10	20.18	24.91	23.42%	0.86	20.23	0.24%	0.92	20.28	0.50%	0.93
Averaged			12.77%	0.85		0.93%	0.93		0.95%	0.93

[a] relative difference of frequency between the measurement and the model.
[b] modal assurance criterion (MAC) of mode shapes between the measurement and the model.